Enhancement of superconductivity far above the critical temperature in double-barrier tunnel junctions

D. R. Heslinga* and T. M. Klapwijk
Department of Applied Physics and Materials Science Centre, University of Groningen, Nijenborgh 4, 9747 AG Groningen, The Netherlands
(Received 4 August 1992)

Motivated by the observation of a superconducting energy gap far above the equilibrium critical temperature T_c in an Al film forming the center electrode of a $Nb/AlO_x/Al/AlO_x/Nb$ structure we analyze the mechanism of gap enhancement in symmetric double-barrier superconducting tunnel junctions. It is found that such structures are very effective in creating a nonthermal distribution of quasiparticles in the middle electrode. At certain bias conditions this leads, according to the BCS gap equation, to the appearance of a nonzero superconducting energy gap even at temperatures up to several times the equilibrium T_c. So the double-barrier arrangement offers the remarkable possibility of making a material become superconducting by applying a voltage or passing a current. Calculated current-voltage characteristics exhibit current steps at voltages $eV=2(\Delta_{Nb}-\Delta_{Al})$ and $eV=2(\Delta_{Nb}+\Delta_{Al})$ in agreement with measured curves. Calculations of the thermodynamic stability of the nonequilibrium superconducting state indicate the possibility of hysteresis effects around these current steps.

I. INTRODUCTION

Enhancement of superconducting properties by driving a superconductor out of thermal equilibrium has been extensively studied in the 1970s. Reviews of experimental and theoretical achievements are given in Refs. 1 and 2. Recently, interest in the subject was revived by the remarkable observation by Blamire *et al.*[3,4] of essentially a zero-temperature energy gap far above the critical temperature T_c in an Al film sandwiched in a symmetric $Nb/AlO_x/Al/AlO_x/Nb$ double-barrier tunnel junction. This is a far stronger effect than observed in previous experiments,[1,2] dramatically illustrating the fact that the vanishing of the superconducting state above a certain T_c is not a consequence of a reduction of the attractive pairing interaction between the electrons, but of the increase of the number of quasiparticle excitations. A preliminary explanation of the phenomena in $Nb/AlO_x/Al/AlO_x/Nb$ junctions[5] was published by us shortly after an early report of the experiment.[3] In the present paper, we give a more elaborate account of the model used in Ref. 5 and its consequences. A theory employing Green's functions was published recently by Zaitsev,[6] who arrived at essentially the same results.

The possibility of gap enhancement is contained in the BCS gap equation. This equation expresses the fact that the energy gap in the quasiparticle excitation spectrum is related to the distribution of quasiparticles over the available energies. With the usual assumptions of an isotropic gap and an energy-independent electron-electron interaction potential V cut off at the Debije frequency ω_D, the BCS equation is written as[7]

$$\frac{1}{N^a(0)V}=\int_{\Delta}^{\hbar\omega_D}\frac{1-2f(E)}{(E^2-\Delta^2)^{1/2}}dE\ . \tag{1}$$

$N^a(0)$ is the unnormalized density of states (DOS) at the Fermi level and $f(E)$ is the quasiparticle distribution function. In equilibrium $f(E)$ equals the thermal Fermi-Dirac function, but Eq. (1) is also valid in a nonequilibrium situation.

At nonzero temperature the magnitude of the energy gap is constrained by the presence of quasiparticles blocking states that would otherwise be available for Cooper pairs. Most important in this respect are the quasiparticles occupying states close to the Fermi level. In Eq. (1) this is reflected by the fact that these energies make the largest contributions to the integral. Gap enhancement can be achieved by removing these quasiparticles, either by extracting them from the material or by redistributing them to higher energies.

This possibility was appreciated by Eliashberg and coworkers,[8–11] who developed a theory of the redistribution mechanism by the use of microwaves with suitable photon energies $h\nu<2\Delta$ and proposed it as an explanation of the critical-current enhancement in microbridges observed several years earlier.[12,13] In subsequent years various experimental approaches to stimulated nonequilibrium superconductivity in more general geometries were developed. Critical-current enhancement in thin Al and Sn films by microwave irradiation was demonstrated by Klapwijk and co-workers[14–16] and Latyshev and Nad.[17] Superconductivity above the equilibrium critical temperature was demonstrated by Klapwijk, Van den Bergh, and Mooij.[15] The redistribution mechanism was also utilized by Gray[18] in symmetric $Al/AlO_x/Al$ SIS (S=superconductor, I=insulator) tunnel junctions. The extraction mechanism was realized by Chang and Scalapino[19] and Chi and Clarke[20] using asymmetric SIS′ junctions, where S′ had a slightly smaller T_c than S. In this work[18–20] asymmetric double-barrier tunnel junctions were used, where the nonequilibrium state was induced by one low-resistance generator junction, while a second high-resistance detector junction was used to measure the

change in the gap.

Despite these successful confirmations of the concept of nonequilibrium-enhanced superconductivity, the observed effects remained small and did not match the theoretical potential. It may be emphasized that superconductivity above the equilibrium critical temperature has only been unequivocally observed in some microwave experiments, the effect being at most 8%.[21]

From this perspective the observation by Blamire *et al.*[4] of a large energy gap at a temperature several times T_c represents a major advance. In this paper we show that their results can be very well reproduced within the context of a simple nonequilibrium SINIS (N=normal metal) model for the double-barrier tunnel junction. The same model has been applied to submicrometer superconductor-semiconductor-superconductor junctions which also satisfy the SINIS scheme.[22] For the present purpose, we simply allow the N layer to be a superconductor with a lower critical temperature than the S electrodes and use Eq. (1) to obtain the nonequilibrium gap.[5] A brief account of the essential features of the experiment by Blamire *et al.*[4] is given in Sec. II. In Sec. III the SINIS model is set forth and the quasiparticle distribution function is derived. In Sec. IV model calculations for Nb/AlO_x junctions are presented. We calculate the distribution function, the dependence of the nonequilibrium Al gap on voltage, temperature, and degree of nonequilibrium, and infer current-voltage (I-V) characteristics which match the experimental ones. The thermodynamic stability of the nonequilibrium superconducting state is considered in Sec. V. Finally, conclusions are given in Sec. VI.

II. MAIN FEATURES OF THE EXPERIMENT

Key elements of the $Nb/AlO_x/Al/AlO_x/Nb$ junctions used by Blamire *et al.*[4] are very thin, highly transmissive tunnel barriers and very thin Al films (3–20 nm). Some measured I-V curves from Ref. 4 are reproduced in Fig. 1. The existence of a superconducting state in the Al middle electrode follows from the presence of current steps at the difference gap voltage $eV=2(\Delta_{Nb}-\Delta_{Al})$ and at the sum gap voltage $eV=2(\Delta_{Nb}+\Delta_{Al})$. These steps are at the same positions as would be expected for a regular SIS'IS tunnel junction where the superconductors S and S' have different gaps. The fact that the current steps persist above T_c of the Al film proves that a gap is still present at these temperatures. If the Al were in the normal state, the structure would behave as a regular SINIS junction with a single gap feature in the I-V curve at $eV=2\Delta_{Nb}$.[22]

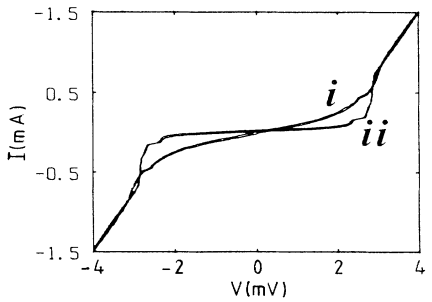

FIG. 1. I-V curves of $Nb/AlO_x/Al/AlO_x/Nb$ tunnel junctions, reproduced from Blamire *et al.* (Ref. 4). The superconducting state in Al is responsible for the small step in the current just below the gap voltage $2\Delta_{Nb}/e$. Curve i, 3-nm Al layer at 4.2 K; curve ii, 12-nm Al layer at 2.2 K.

It is essential to observe that not only does the nonequilibrium gap in Al show up in the I-V curve around the gap voltage of the adjoining Nb electrodes, but in fact it only *exists* in the voltage range between $2(\Delta_{Nb}-\Delta_{Al})$ and $2(\Delta_{Nb}+\Delta_{Al})$. As will be shown below, only there is the quasiparticle extraction sufficiently effective.

The extraordinary magnitude of the enhancement effect is due to the optimal conditions for quasiparticle extraction achieved in these junctions. The symmetry of the structure, which approaches an original scheme devised by Parmenter,[23] ensures equal reduction of electronlike and holelike quasiparticles. Furthermore, the large gap of the Nb electrodes enables removal of quasiparticles over a large energy range. The high transmissivity of the tunnel barriers and the very thin Al films promote fast extraction of quasiparticles from the film and establishment of a nonequilibrium situation. Finally, this nonequilibrium is maintained relatively easily in Al because inelastic relaxation is exceptionally slow.[24]

III. SINIS MODEL

The SINIS model takes advantage of the symmetry of the double-barrier structure of the junctions to arrive at the distribution function $f_2(E)$ in the middle electrode.[22] Assuming identical tunnel barriers and identical left and right superconductors, the situation is as in Fig. 2, with the junction voltage distributed equally over the two interfaces. In the figure the middle electrode 2 is represented in the normal state. In the case of an Al film above its equilibrium critical temperature, it is not *a priori* known whether the middle electrode is in fact normal or superconducting, but the following derivation is valid in both cases. Because of the symmetry of the arrangement, charge imbalance does not occur and the mixed nature of the injected quasiparticles will be ignored. It is assumed that the superconducting electrodes 1 and 3 remain in

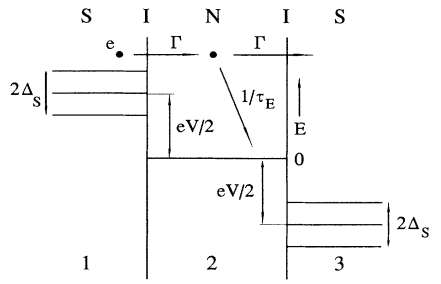

FIG. 2. SINIS model of a double-barrier tunnel structure. V is the junction voltage, Γ denotes the injection of carriers into the middle electrode, and $1/\tau_E$ the energy relaxation of injected carriers.

equilibrium and the occupation of states is determined by the Fermi-Dirac (FD) distribution f_0 at the bath temperature. States in electrode 2 are populated from electrode 1, while depopulation occurs either by extraction into electrode 3 or by inelastic relaxation toward the FD distribution. The resulting occupation function f_2 in steady state can be found by equating, for each energy level, the population and depopulation rates. Elastic scattering in electrode 2 does not change the energy distribution and is not explicitly included in the model.

According to the Fermi golden rule, the current of electrode 1 to 2 is written as[25] (the energy E is measured from the Fermi level in electrode 2)

$$I=\frac{2e}{R_N}\int_{-\infty}^{\infty} N_1(E-eV/2)N_2(E) \times[f_0(E-eV/2)-f_2(E)]dE \ , \tag{2}$$

with $N_{1,2}$ the density of states normalized to the value at the Fermi level in the normal state and R_N the normal-state resistance of the double-barrier junction, i.e., twice the resistance of a single barrier,

$$\frac{R_N}{2}=\frac{\hbar}{2\pi A|T|^2N_1^a(0)N_2^a(0)}=\frac{R_c}{A} \ . \tag{3}$$

A is the junction area, $|T|^2$ the transmission coefficient, $N_{1,2}^a$ the absolute, *unnormalized* DOS, and R_c the specific contact resistance of the single barrier.

The population rate at a certain energy level is just the current at that level divided by the electronic charge,

$$\frac{2}{R_N}N_1(E-eV/2)N_2(E)[f_0(E-eV/2)-f_2(E)] \ . \tag{4}$$

Analogously, the extraction rate from electrode 2 to 3 is

$$\frac{2}{R_N}N_2(E)N_3(E+eV/2)[f_2(E)-f_0(E+eV/2)] \ . \tag{5}$$

We treat the inelastic relaxation of injected hot carriers by a simple relaxation-time model. The relaxation rate at the energy level E is given by

$$ALN_2^a(E)e^2\frac{f_2(E)-f_0(E)}{\tau_E} \ , \tag{6}$$

where L is the thickness of electrode 2. Formally, τ_E is the relaxation time of the energy distribution function with respect to the FD distribution at the bath temperature. τ_E is assumed not to depend on energy or on the magnitude of the deviation from the equilibrium. A further assumption is that the phonon distribution remains in thermal equilibrium.

The steady-state occupation of the level E is determined by the balance Eq. (4) = Eq. (5) + Eq. (6). After some rearranging we get the distribution function in electrode 2,

$$f_2(E)=\frac{N_1(E-eV/2)f_0(E-eV/2)+N_3(E+eV/2)f_0(E+eV/2)+\dfrac{N_2(E)f_0(E)}{\Gamma\tau_E}}{N_1(E-eV/2)+N_3(E+eV/2)+\dfrac{N_2(E)}{\Gamma\tau_E}} \ , \tag{7}$$

where Γ is the tunneling injection rate into region 2, defined as the number of particles injected per second normalized to the number of available states in the volume under consideration,

$$\Gamma=\frac{1}{N_2^a(0)R_cLe^2} \ . \tag{8}$$

When the injection rate exceeds the relaxation rate, $\Gamma\tau_E\gg1$; f_2 differs considerably from the equilibrium FD distribution. For $\Gamma\tau_E\ll1$, equilibrium is recovered, $f_2=f_0$. According to Eq. (7), $f_2(E)$ depends on the DOS $N_2(E)$, which in turn depends on the magnitude of the (nonequilibrium) energy gap. So, to find both the gap and distribution function, Eqs. (1) and (7) have to be solved self-consistently.

The current through the first tunnel barrier is obtained by inserting Eq. (7) into Eq. (2). The same current passes through the second barrier. If $\Gamma\tau_E=0$, Eq. (2) reduces to the well-known SIN tunneling expression. In the absence of inelastic relaxation, $\Gamma\tau_E\to\infty$; the current simplifies to

$$I=\frac{2e}{R_N}\int_{-\infty}^{\infty}\frac{N_1(E-eV/2)N_2(E)N_3(E+eV/2)}{N_1(E-eV/2)+N_3(E+eV/2)} \times[f_0(E-eV/2)-f_0(E+eV/2)]dE \ . \tag{9}$$

Clearly, this expression is different from both SIN and SIS tunneling.[25]

Having introduced the notions of quasiparticle injection and extraction, it is easy to grasp qualitatively at which junction voltages a nonequilibrium gap in the middle electrode will be possible. This is illustrated by Fig. 3, where for simplicity it is assumed that there is no relaxation. Figure 3(a) depicts the situation at low voltages, $eV<2(\Delta_{Nb}-\Delta_{Al})$. Because the quasiparticles in the electronlike branch in the energy range $0-(\Delta_{Nb}-eV/2)$ are blocked by the gap of the right S electrode, they are not extracted [the same is true for the quasiholes in the range $-(\Delta_{Nb}-eV/2)-0$] and no gap develops. In between the two characteristic voltages $2(\Delta_{Nb}-\Delta_{Al})<eV<2(\Delta_{Nb}+\Delta_{Al})$, shown in Fig. 3(b), the extraction is sufficiently effective and by developing a gap $\approx\Delta_{Al}(0)$ the Al can either push out to the right those quasiparticles remaining in the range $0-(\Delta_{Nb}-eV/2)$ [if $2(\Delta_{Nb}-\Delta_{Al})<eV<2\Delta_{Nb}$] or keep out those trying to enter from the left in the range $0-(eV/2-\Delta_{Nb})$ [if $2\Delta_{Nb}<eV<2(\Delta_{Nb}+\Delta_{Al})$]. At large voltages $eV>2(\Delta_{Nb}+\Delta_{Al})$ [Fig. 3(c)], the Al gap is too small to keep out the quasiparticles entering from the left and the gap is quenched. In short, it is only in the range $2(\Delta_{Nb}-\Delta_{Al})<eV<2(\Delta_{Nb}+\Delta_{Al})$ that a none-

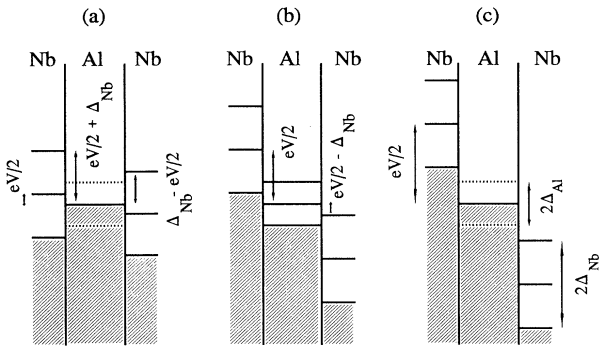

FIG. 3. A nonequilibrium gap in the Al middle electrode can only exist in a limited voltage range. The figures are drawn neglecting the thermal broadening of the electron distribution. (a) $eV<2(\Delta_{Nb}-\Delta_{Al})$, no gap possible; the dashed line indicates the magnitude of the (zero-temperature) Al gap; (b) $2(\Delta_{Nb}-\Delta_{Al})<eV<2(\Delta_{Nb}+\Delta_{Al})$, a gap can be maintained; (c) $eV>2(\Delta_{Nb}+\Delta_{Al})$, no gap possible.

quilibrium gap can exist.

In all three cases at nonzero temperature, a few quasiparticles are injected above the energy gap of the left electrode at $E>eV/2+\Delta_{Nb}$, but these are far from the Fermi level and have minimal weight in the BCS integral. This implies that once a gap is possible it will have only a small dependence on voltage. The largest gap will occur at the highest possible voltage when the few remaining quasiparticles are furthest from the Fermi energy. The opinion of Blamire *et al.*[4] that the maximum gap occurs at what they call "the maximum extraction condition" $eV=2(\Delta_{Nb}-\Delta_{Al})$ is incorrect.

IV. CALCULATED RESULTS

Using Eq. (8), we can check whether the $Nb/AlO_x/Al/AlO_x/Nb$ stack satisfies the condition for nonequilibrium, $\Gamma\tau_E\geq 1$. The experimental[4] R_c was $3-7\times10^{-11}\ \Omega\,m^2$. Calculating $N_{Al}(0)$ using free-electron formulas and textbook values[26] $n=18.1\times10^{22}\ cm^{-3}$ and $E_F=11.7$ eV for the carrier concentration and the Fermi energy, we find for a film thickness of 10 nm an injection rate $\Gamma\sim5\times10^8\ s^{-1}$. With an inelastic relaxation time estimated[24] on the order of 10^{-8} s at T_c, we get $\Gamma\tau_E\sim1$. This is high enough to expect some gap enhancement, but apparently the degree of nonequilibrium is not extreme.

For the calculations we take Nb with $T_c=9.25$ K and $\Delta(0)=1.52$ meV (Ref. 27) for electrodes 1 and 3 and a resistance of 1 Ω for a single interface, and so $R_N=2\ \Omega$. For the Al films, we take a constant DOS $N_2(E)=1$ and bulk parameters $T_c=1.18$ K, $\Delta_{Al}(0)=0.166$ meV,[27] and $N^a(0)V=0.167$.[7] We note that in the experiments of Blamire *et al.*[4] the equilibrium T_c of Al was higher than the bulk value and ranged up to ~2.4 K, as is common for thin Al films.

To illustrate the basic mechanism of quasiparticle extraction, we first show the nonequilibrium distribution function of a middle electrode remaining in the normal state, and so we turn off the attractive pairing interaction and fix Δ_{Al} to zero. The distribution function f_2 at 4.2 K for various values of the parameter $\Gamma\tau_E$ is plotted in Fig. 4 for voltage $eV=3.04$ meV, which is slightly higher than $2\Delta_{Nb}=2.96$ meV at this temperature. The net reduction of excited carriers for increasing values of $\Gamma\tau_E$ is clearly visible. Those states in electrode 2 above the Fermi level ($E>0$) lying opposite the gap in electrode 1 are depopulated because there is no injection. Those below the Fermi level ($E<0$) lying opposite the gap in electrode 3 are overpopulated (i.e., the number of holes is reduced) because there is no extraction. Thus, at nonzero voltage, the effect on the number of excited quasiparticles in these ranges is similar to a lowering of the temperature. The peaked structures directly adjacent to these ranges are caused by the divergence typical of the BCS density of states in electrodes 1 and 3. When $eV<2\Delta$ (not shown), there is an energy range around the Fermi level where the gaps in electrodes 1 and 3 overlap and the FD distribution is retained.

As an aside, we point out the effect of the nonequilibrium distribution on the current.[22] Because the levels opposite the gap in either electrode 1 or 3 only communicate with one of the superconducting electrodes, in the limit of extreme nonequilibrium they cannot carry current from electrode 1 to 3. For intermediate $\Gamma\tau_E$ their participation in the conduction process is partially restored. In Ref. 22 it was shown that this reduction of the range of current-carrying energy levels leads to a smaller current compared to the equilibrium situation. In the asymptotic limit $eV>\Delta$, this so-called *current deficit* reaches a constant, voltage-independent value which depends on $\Gamma\tau_E$ and essentially scales with the energy gap of the superconducting electrodes as a function of temperature. We emphasize that the current deficit is a consequence of the presence of an energy gap in electrodes 1 and 3. Were they in the normal state, the energy distribution of electrons in electrode 2 would still deviate from equilibrium, but it would leave the I-V characteristic unaffected because all levels would fully participate in the transport of current.

Next, we turn on the pairing interaction in the middle electrode and allow the Al to develop an energy gap determined by Eq. (1) when the nonequilibrium is strong enough. The effect on the distribution function f_2 for energies above the Fermi level is shown in Fig. 5 for several

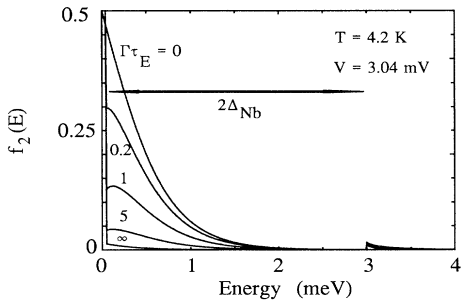

FIG. 4. Distribution function f_2 for different degree of nonequilibrium with the Al gap set to zero, $eV=3.04$ meV $>2\Delta_{Nb}$, $T=4.2$ K. For the equilibrium case, $\Gamma\tau_E=0$; f_2 is equal to the thermal Fermi-Dirac (FD) distribution.

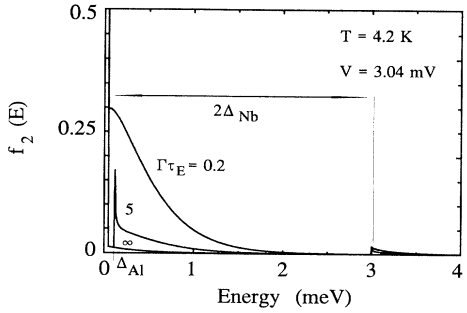

FIG. 5. Distribution function f_2 for different degree of nonequilibrium, $eV=3.04$ meV $>2\Delta_{Nb}$, $T=4.2$ K. For large $\Gamma\tau_E$ (shown for $\Gamma\tau_E=5$), the BCS density of states in the superconducting Al layer gives rise to a peak in f_2 at energy $E=\Delta_{Al}$. For $\Gamma\tau_E=\infty$, the Al is also superconducting, but the peak is not visible. If $\Gamma\tau_E$ is too small (shown for $\Gamma\tau_E=0.2$), the Al is not superconducting and the situation is identical to Fig. 3.

values of $\Gamma\tau_E$, again for $T=4.2$ K and $V=3.04$ mV as in Fig. 4. Note that this voltage is in between $2\Delta_{Nb}$ and $2[\Delta_{Nb}+\Delta_{Al}(0)]$. The difference with Fig. 4 when nonequilibrium is strong enough and when a gap exists in Al is mainly in the narrow range between $E=0$ and Δ_{Al}, where f_{Al} is strongly reduced because $N_{Al}=0$ in Eq. (7). When $\Gamma\tau_E$ becomes too small, the gap in Al disappears and the situation of Fig. 4 is recovered. As before, a tiny peak of injected quasiparticles occurs at $eV/2+\Delta_{Nb}$.

Figure 6 shows the Al gap as a function of voltage at 4.2 K for various $\Gamma\tau_E$. At the low and high ends of the voltage range where Δ_{Al} exists, there are two solutions of Eq. (1). The meaning of the two lower branches will be clarified in Sec. V. For now, we concentrate on the upper branch. For large $\Gamma\tau_E$ this branch almost equals the zero-temperature gap $\Delta_{Al}(0)$ even though the temperature is several times the equilibrium T_c, and so indeed the large enhancement of the Al gap is reproduced convincingly. Both the magnitude of Δ_{Al} and the voltage range where it exists decrease with weakening nonequilibrium. As anticipated above, the voltage dependence is rather weak. For stong nonequilibrium Δ_{Al} increases slightly with voltage, as expected. However, for low $\Gamma\tau_E$ the variation $d\Delta_{Al}/dV$ is negative. This is because for smaller $\Gamma\tau_E$ the effect on the BCS integral of the shifting to higher energy of the peak in $f_2(E)$ of quasiparticles injected above $eV/2+\Delta_{Nb}$ when the junction voltage is increased is outweighed by the increase of the voltage range closer to E_F where the FD distribution is approached.

In Fig. 7 the Al gap at $eV=2\Delta_{Nb}=2.96$ meV is plotted as a function of $\Gamma\tau_E$ at 4.2 K. Obviously, in the extreme limits $\Gamma\tau_E\ll1$ ($\Delta_{Al}=0$) and $\Gamma\tau_E\gg1$ [$\Delta_{Al}\approx\Delta_{Al}(0)$], there is little variation in Δ_{Al}. Only in the transition region between 0.1 and 10 is the gap strongly dependent on the degree of nonequilibrium. The fact that in the experiment the current step was observed to shift to a higher voltage for larger Al thickness,[4] i.e., lower Γ, implies that the Al films were in this transitional regime, consistent with the estimate of $\Gamma\tau_E$ made above.

In Fig. 8 the temperature dependence of Δ_{Al} at $eV=2\Delta_{Nb}(T)$ is plotted for various $\Gamma\tau_E$. In the range between the critical temperatures of Al and Nb, the temperature dependence is weak and a gap persists almost to the critical temperature of the Nb electrodes. For extreme nonequilibrium Δ_{Al} remains essentially constant up to a temperature several times the equilibrium T_c and only starts to decline as the gap of the adjoining Nb electrodes shrinks, because that brings the injected quasiparticles closer to the Fermi energy in the Al. This predicted behavior may be compared with the measured $\Delta_{Al}(T)$ from Ref. 4, which is reproduced in Fig. 9. Unfortunately, the measurement covers only a small temperature range, but it appears consistent with the calculated curves for intermediate $\Gamma\tau_E$.

Finally, we show some calculated I-V curves in Fig. 10, where the 2×SIN curve is also shown for comparison. The curve for extreme nonequilibrium ($\Gamma\tau_E\to\infty$) with the calculated Δ_{Al} of the upper branch of Fig. 6 and the one with Δ_{Al} deliberately set to zero are equal at voltages where Eq. (1) has no solution. However, in the range where Δ_{Al} is nonzero, the current remains low up to $eV=2(\Delta_{Nb}+\Delta_{Al})$. This effect distinguishes a SINIS junction with a low-temperature superconductor as middle electrode from a junction with a nonsuperconductor. The current jump at $eV=2(\Delta_{Nb}+\Delta_{Al})$ is real and not an artifact of the calculation. It is a consequence of the discontinuous jump to zero of Δ_{Al} at this voltage. The intermediate curve for $\Gamma\tau_E=2$ has a smaller current deficit

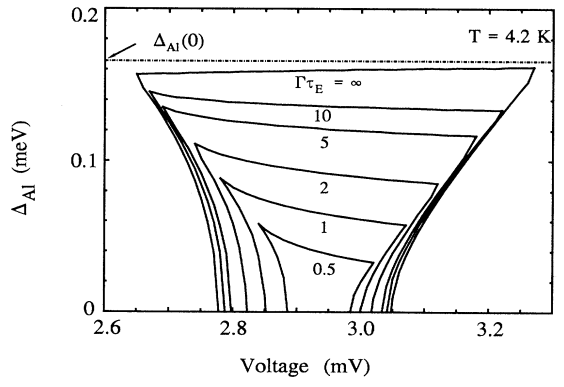

FIG. 6. Energy gap in Al as a function of voltage for different $\Gamma\tau_E$, $T=4.2$ K.

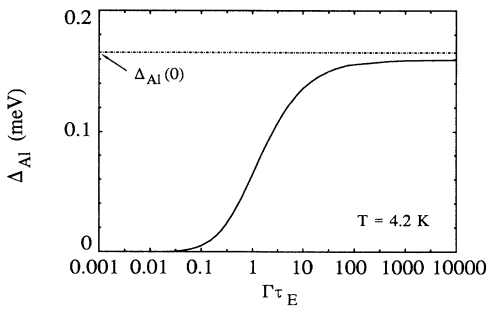

FIG. 7. Energy gap in Al as a function of $\Gamma\tau_E$, $T=4.2$ K, $eV=2.96$ meV $=2\Delta_{Nb}$.

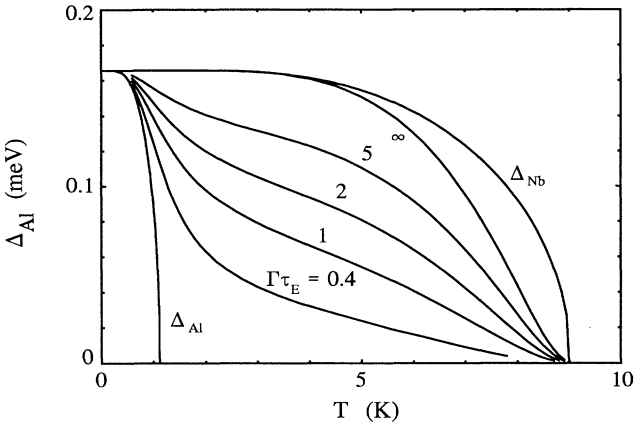

FIG. 8. Energy gap in Al as a function of temperature for different $\Gamma\tau_E$ at $eV=2\Delta_{Nb}(T)$. The BCS temperature dependence of Δ_{Nb} and Δ_{Al}, both scaled to $\Delta_{Al}(0)$, is also shown for comparison.

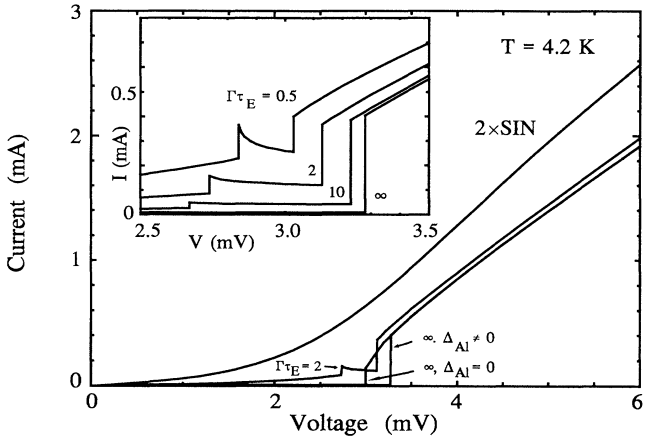

FIG. 10. Calculated I-V curves showing the current steps at $eV=2(\Delta_{Nb}-\Delta_{Al})$ and $2(\Delta_{Nb}+\Delta_{Al})$ due to superconductivity in Al.

than those for $\Gamma\tau_E=\infty$ and a clearly distinguishable step in the current below $eV=2\Delta_{Nb}$.

The inset to Fig. 10 shows the region around $eV=2\Delta_{Nb}$ in more detail for various $\Gamma\tau_E$. The experimentally observed step is reproduced at the voltage $eV=2(\Delta_{Nb}-\Delta_{Al})$ and thus shifts to a higher voltage for lower $\Gamma\tau_E$, while the step at $2(\Delta_{Nb}+\Delta_{Al})$ moves inward. The height of the subgap step has a peculiar dependence on the degree of nonequilibrium. The step is due to current carried by electrons at the level $E=\Delta_{Al}$ in the middle electrode. For that, the level needs to be populated, and as this cannot occur through direct injection but only through energy loss of the injected carriers, the step will be larger when the inelastic relaxation is stronger. Indeed, some relaxation has to be present for the current step to be observable at all, and so we have the paradoxical result that whereas stronger nonequilibrium promotes the superconducting state in Al, it cannot be detected in the extreme limit. Figure 10 also reveals the occurrence of a negative differential resistance next to the subgap step. In a current-biased measurement as performed in Ref. 4, this will result in a horizontal jump in the recorded characteristic, which indeed appears to be what is observed (cf. Fig. 1).

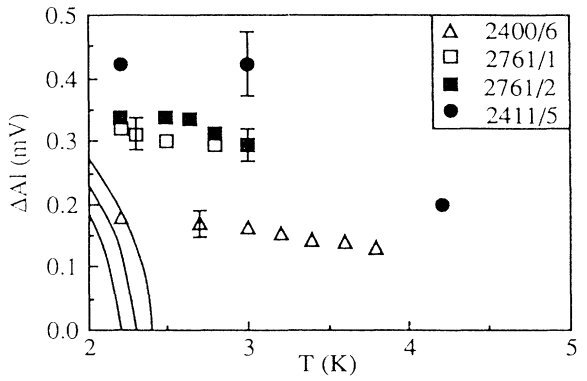

FIG. 9. Measured Al energy gap in Nb/AlO_x/Al/AlO_x/Nb tunnel junctions as a function of temperature (reproduced from Ref. 4). Solid lines show the BCS temperature dependence of the equilibrium gaps with the experimental equilibrium T_c of the Al layer.

V. FREE ENERGY AND THE I-V CHARACTERISTIC

We now proceed to explain the occurrence of two solutions of the BCS equation (1) in certain voltage ranges. To this end we observe that Eq. (1) determines a situation where the free energy F of the system is minimized, i.e., $dF/d\Delta=0$. This condition can, of course, also describe a maximum in F, which as we shall see is in fact the meaning of the second solution for Δ. The free energy can be obtained by integrating the BCS equation

$$F(\Delta)=-\frac{1}{N(0)V}-\int_0^{\Delta}d\Delta'\int_{\Delta}^{\hbar\omega_D}\frac{1-2f_2(E)}{(E^2-\Delta'^2)^{1/2}}dE\ . \tag{10}$$

In Ref. 28 a Ginzburg-Landau approximation to Eq. (10) was developed, but since we do not have a situation with small gaps, we calculate the integral numerically.

The free energy as a function of Δ_{Al} for various junction voltages is plotted in Fig. 11 for the case $\Gamma\tau_E\rightarrow\infty$ and $T=4.2$ K. Below $eV=2(\Delta_{Nb}-\Delta_{Al})$ (we will call this region I), Eq. (1) has no solution and F is a monotonously rising function. Above $eV=2(\Delta_{Nb}-\Delta_{Al})$, Eq. (1) has two solutions. The smaller Δ_{Al} corresponds to a local maximum of F, the larger one to a minimum. At first, this is a local minimum and the superconducting state is not globally stable (region II), but as V rises, it rapidly develops into a global minimum (region III). This corresponds to the steep decline of the lower branches in Fig. 6. In region IV only one solution of Eq. (1) remains and F is negative for all Δ_{Al}. At yet higher voltages, the reverse sequence is followed through regions V (two solutions, global minimum) and VI (two solutions, local minimum) until finally a solution of Eq. (1) no longer exists and F rises monotonously as for low voltages (region VII).

So the upper branches in Fig. 6 represent a minimum

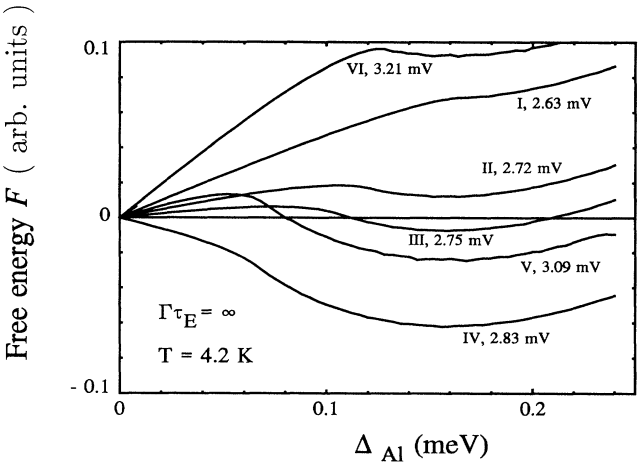

FIG. 11. Free energy F of Al as a function of the energy gap at different junction voltages, $\Gamma\tau_E=\infty$, $T=4.2$ K. The divisions into the regions I–VI is explained in the text.

in the free energy of Al in the superconducting state, but this does not imply that the system will always be superconducting. In regions II and VI where the superconducting state is not globally stable, this is evident. In regions III and V, the superconducting state is thermodynamically stable, but the system has to overcome an energy barrier when it is initially in the normal state. Consequently, in these regions the actual thermodynamic state depends on the history of the system. Only in region IV is the Al certainly superconducting.

These considerations imply that the I-V characteristics in Fig. 10 are deceptive. Starting from $V=0$, we have let the Al jump to the superconducting state as soon as region II was entered and let it jump back to the normal state only as region VI was left. In reality, the picture is more complicated, as illustrated in Fig. 12 for the case $\Gamma\tau_E=\infty$ and $T=4.2$ K. As V increases, the Al is not superconducting in region II, while it definitely is in region

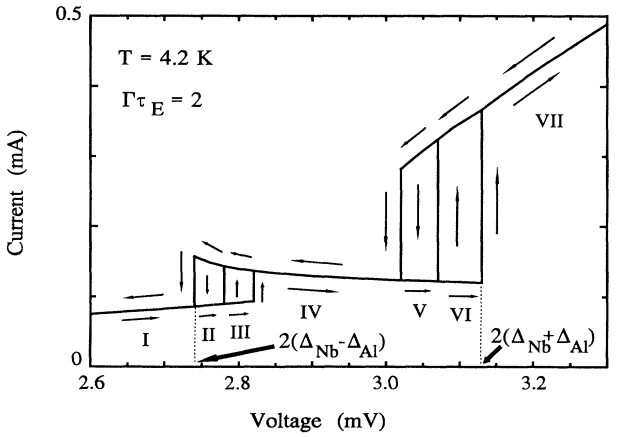

FIG. 12. I-V curve for $\Gamma\tau_E=2$, $T=4.2$ K, showing hysteresis effects around regions II–III and V–VI. The arrows indicate the way the curve is traced in a current-biased experiment. The location of the current steps is not fixed.

IV. The jump to the superconducting state occurs somewhere in the intermediate region III, but since this is a probabilistic process, the corresponding step in the I-V characteristic is not at a fixed voltage. Experimentally, this may be hard to see because region III is quite narrow. As the voltage is further increased, the Al will remain superconducting at least until region VI is entered. Somewhere in region VI the system jumps back to the normal state, but again the voltage at which the jump in the I-V characteristic occurs is not fixed. Finally, in region VII the system is normal. Scanning the voltage in the opposite direction gives a slightly different picture. The Al now remains normal in the region VI, and the jump to the superconducting state occurs somewhere in region V. Likewise, the superconducting state is maintained through region III and the system reverses to the normal state somewhere in region II.

As a result, hysteresis could occur at both steps in the I-V characteristic. Consequently, the labeling of the voltages where the jumps occur given in Ref. 4 and in the previous section must be modified. The subgap step appears not at $eV=2(\Delta_{Nb}-\Delta_{Al})$, but at slightly higher voltage. The second step does not appear at $eV=2\Delta_{Nb}$, as assumed by Blamire *et al.*,[4] nor at $eV=2(\Delta_{Nb}+\Delta_{Al})$, as suggested in Fig. 10, but somewhere in between.

We should point out that the hysteresis effects predicted here are different from the hysteresis and various jumps in the I-V curve reported in subsequent experiments with $Nb/AlO_x/Al/AlO_x/Nb$ junctions.[29] The latter are observed only below the equilibrium T_c of the Al layer where supercurrents occur in addition to a nonequilibrium distribution of quasiparticles. This is outside the scope of the present discussion.

VI. SUMMARY AND CONCLUSIONS

We have discussed the mechanism of energy-gap enhancement in superconductors within the context of a simple symmetric SINIS double-barrier tunneling model under the conditions of high interface transmission and weak inelastic scattering. Depending on the balance between injection and energy relaxation, a nonequilibrium energy distribution of electrons in the middle N region occurs. When the middle electrode is in the normal state, this leads to a current deficit at asymptotic voltages, which scales with the superconducting energy gap as a function of temperature.

When the middle electrode is a superconductor S′ with a low critical temperature, a nonequilibrium energy gap in the quasiparticle excitation spectrum can develop. The gap enhancement is calculated by solving the equation for the nonequilibrium distribution function and the BCS gap equation self-consistently. We have calculated the dependence of the nonequilibrium gap on junction voltage, temperature, and nonequilibrium conditions for $Nb/AlO_x/Al/AlO_x/Nb$ tunnel junctions. It is found that an energy gap can be sustained up to temperatures several times the equilibrium T_c, thereby confirming the recent experimental observations of such a large effect.

Calculated I-V curves reproduce well the current steps occurring in the measured characteristics near the

characteristic voltages $2(\Delta_{Nb}-\Delta_{Al})$ and $2(\Delta_{Nb}+\Delta_{Al})$. The original analysis given in previous papers[3-5] is refined and supplemented by including considerations concerning the thermodynamic stability of the nonequilibrium superconducting state. A possible small hysteresis effect near the two step voltages is predicted. More extensive gap measurements would provide interesting testing materials for the present model.

As the SINIS configuration proves very effective in extracting quasiparticles, we may consider the recurring question as to what limits the temperature up to which a nonequilibrium superconducting gap can be sustained. From the above three essential features for achieving a large effect can be identified: (i) a large gap in the outer S electrodes to be able to sweep out the quasiparticles over a large energy range, (ii) a high injection and extraction rate, and (iii) slow inelastic relaxation in the middle electrode. It is a fortunate coincidence that the development of a well-controlled Nb tunnel junction technology has produced as a by-product $Nb/AlO_x/Al/AlO_x/Nb$ junctions that turn out to be virtually completely optimized on all these three points. In fact, it is hard to imagine a better junction design if one sticks to low-temperature superconductors.

However, it can be seen from the BCS equation that the temperature in itself is not a limiting factor for gap enhancement, assuming that the strength of the pairing interaction remains unchanged. Consequently, it should in principle be possible to achieve gap enhancement at even much higher temperatures by using a material with a much larger gap than Nb for the outer electrodes. High-T_c superconductors and even semiconductors are obvious candidates. The latter are particularly advantageous because they offer large gaps of the order of ~ 1 eV. This scheme has in fact been envisaged as far back as 1973 by Aronov and Gurevich.[30] With the immense progress in semiconductor fabrication technology since then, the fascinating prospect of such a semiconductor-superconductor-semiconductor junction appears now within reach.

ACKNOWLEDGMENTS

We thank M. G. Blamire for stimulating discussions. This work was supported by the Netherlands Organization for Scientific Research (NWO) through the Foundation for Fundamental Research on Matter (FOM).

*Present address: Department of Experimental Physics, Research Institute for Materials, University of Nijmegen, Toernooiveld, 6525 ED Nijmegen, The Netherlands.

[1]J. E. Mooij, in *Nonequilibrium Superconductivity, Phonons, and Kapitza Boundaries,* edited by K. E. Gray (Plenum, New York, 1981), p. 191; K. E. Gray, in *ibid.*, p. 131.

[2]V. M. Dmitriev, V. N. Gubankov, and F. Y. Nad, in *Nonequilibrium Superconductivity,* edited by D. N. Langenberg and A. I. Larkin, Vol. 12 of *Modern Problems in Condensed Matter Physics,* edited by V. M. Agranovich and A. A. Maradudin (North-Holland, Amsterdam, 1986), p. 163; G. M. Eliashberg and B. I. Ivlev, in *ibid.* p. 211.

[3]M. G. Blamire, E. C. G. Kirk, J. E. Evetts, and T. M. Klapwijk, Physica B **165/166**, 1583 (1990).

[4]M. G. Blamire, E. C. G. Kirk, J. E. Evetts, and T. M. Klapwijk, Phys. Rev. Lett. **66**, 220 (1991).

[5]T. M. Klapwijk, D. R. Heslinga, and M. G. Blamire, Physica B **165/166**, 1579 (1990).

[6]A. V. Zaitsev, Pis'ma Zh. Eksp. Teor. Fiz. **55**, 66 (1992) [JETP Lett. **55**, 67 (1992)].

[7]A. L. Fetter and J. D. Walecka, *Quantum Theory of Many-Particle Systems* (McGraw-Hill, New York, 1971).

[8]G. M. Eliashberg, Pis'ma Zh. Eksp. Teor. Fiz. **11**, 186 (1970) [JETP Lett. **11**, 114 (1970)]

[9]G. M. Eliashberg, Zh. Eksp. Teor. Fiz. **61**, 1254 (1971) [Sov. Phys. JETP **34**, 668 (1972)].

[10]B. V. Ivlev and G. M. Eliashberg, Pis'ma Zh. Eksp. Teor. Fiz. **13**, 464 (1971) [JETP Lett. **13**, 333 (1973)].

[11]B. V. Ivlev, S. G. Lisitsyn, and G. M. Eliashberg, J. Low Temp. Phys. **10**, 449 (1973).

[12]A. F. G. Wyatt, V. M. Dmitriev, W. S. Moore, and F. W. Sheard, Phys. Rev. Lett. **16**, 1166 (1966).

[13]A. H. Dayem and J. J. Wiegand, Phys. Rev. **155**, 418 (1967).

[14]T. M. Klapwijk and J. E. Mooij, Physica B **81**, 132 (1976).

[15]T. M. Klapwijk, J. N. van den Bergh, and J. E. Mooij, J. Low Temp. Phys. **26**, 385 (1977).

[16]J. E. Mooij, N. Lambert, and T. M. Klapwijk, Solid State Commun. **36**, 585 (1980).

[17]Y. I. Latyshev and F. Y. Nad, IEEE Trans. Magn. **MAG-11**, 877 (1975); Zh. Eksp. Teor. Fiz. **71**, 2158 (1976) [Sov. Phys. JETP **44**, 1136 (1976)].

[18]K. E. Gray, Solid State Commun. **26**, 633 (1978).

[19]J. J. Chang and D. J. Scalapino, J. Low Temp. Phys. **29**, 477 (1977); J. J. Chang, Phys. Rev. B **11**, 20 (1978).

[20]C. C. Chi and J. Clarke, Phys. Rev. B **20**, 4465 (1979).

[21]J. A. Pals and J. Dobben, Phys. Rev. B **20**, 935 (1979).

[22]D. R. Heslinga, W. M. van Huffelen, and T. M. Klapwijk, IEEE Trans. Magn. **MAG-27**, 3264 (1991).

[23]R. H. Parmenter, Phys. Rev. Lett. **11**, 274 (1961).

[24]S. B. Kaplan, C. C. Chi, D. N. Langenberg, J. J. Chang, S. Jafaney, and D. J. Scalapino, Phys. Rev. B **14**, 4854 (1976).

[25]E. L. Wolf, *Principles of Electron Tunneling Spectroscopy* (Oxford University Press, New York, 1985).

[26]N. W. Ashcroft and N. D. Mermin, *Solid State Physics* (Holt, Rinehart & Winston, New York, 1976).

[27]T. Van Duzer and C. W. Turner, *Principles of Superconductive Devices and Circuits* (Elsevier, New York, 1981).

[28]A. Schmid, Phys. Rev. Lett. **38**, 922 (1977); U. Eckern, A. Schmid, M. Schmutz, and G. Schön, J. Low Temp. Phys. **36**, 643 (1979).

[29]M. G. Blamire, E. C. G. Kirk, R. E. Somekh, and J. E. Evetts, IEEE Trans. Magn. **MAG-27**, 2598 (1991).

[30]A. G. Aronov and V. L. Gurevich, Zh. Eksp. Teor. Fiz. **63**, 1809 (1972) [Sov. Phys. JETP **36**, 957 (1973)].